NASA TECHNICAL MEMORANDUM

NASA TM X-73424

NASA TM X-73424

(NASA-TM-X-73424) AERODYNAMIC AND ACOUSTIC PERFORMANCE OF A CONTRACTING COWL HIGH THROAT MACH NUMBER INLET INSTALLED ON NASA QUIET ENGINE C (NASA) 20 p HC $3.50 CSCL 01A G3/02

N76-27168

Unclas 42394

AERODYNAMIC AND ACOUSTIC PERFORMANCE OF A CONTRACTING COWL HIGH THROAT MACH NUMBER INLET INSTALLED ON NASA QUIET ENGINE "C"

by Harry E. Bloomer and John W. Schaefer
Lewis Research Center
Cleveland, Ohio 44135

TECHNICAL PAPER to be presented at
Third Aero-Acoustics Conference sponsored by
the American Institute of Aeronautics and Astronautics
Palo Alto, California, July 20-23, 1976

AERODYNAMIC AND ACOUSTIC PERFORMANCE OF A CONTRACTING COWL HIGH THROAT MACH NUMBER INLET INSTALLED ON NASA QUIET ENGINE "C"

Harry E. Bloomer and John W. Schaefer
National Aeronautics and Space Administration
Lewis Research Center
Cleveland, Ohio 44135

Abstract

The purpose of this experimental program was to evaluate the approach and takeoff performance of a contracting-cowl variable geometry design inlet installed on a high-bypass-ratio turbofan engine. The design was finalized after consideration of aerodynamic, acoustic, and mechanical factors which would lead to a viable flight-worthy inlet concept. The aerodynamic results are presented in terms of inlet recovery and distortion parameter as functions of throat Mach number, and acoustic results in terms of Perceived Noise Level. The contracting cowl high throat Mach number inlet is shown to be an attractive means to reduce forward radiated noise from a high bypass ratio turbofan engine.

Introduction

To achieve turbofan inlet noise reductions, many types of sonic and near-sonic variable-geometry inlet configurations have been proposed. Of all the inlet concepts studied for CTOL application, the contracting cowl configuration was considered to be the best compromise from the standpoint of mechanical, aerodynamic, and acoustic design potential. The purpose of the experimental program reported herein was to evaluate the approach and takeoff performance of a contracting-cowl variable-geometry design inlet installed on a high-bypass-ratio turbofan engine.

NASA's Quiet Engine "C" was selected for tests of the high Mach number inlet. The inlet design was finalized by the engine contractor and reviewed and approved by NASA personnel after consideration of aerodynamic, acoustic, and mechanical factors which would lead to a viable flight-worthy inlet concept. The design procedure used on a similar inlet by the same contractor is reported in Ref. 1. Some previous work on various high throat Mach number inlet concepts is reported in Refs. 2 to 6.

To minimize costs of the test hardware fixed-geometry approach and takeoff inlet contours conforming to the postulated variable geometry design were fabricated. They were installed on Quiet Engine "C" and tested at static conditions in the Engine Noise Test Facility of the NASA-Lewis Research Center. The approach and takeoff high Mach number inlet configurations were run over a range of throat Mach numbers from about 0.5 to choked by varying corrected fan speed. Both aerodynamic and acoustic data were obtained, analyzed, and compared to data obtained with a baseline cylindrical inlet which had a bellmouth to assure smooth inflow conditions to the engine. Empirical inlet surface Mach number distributions as well as flow variations are compared to results from an analytical program.[7] Some operational problem aspects of using high Mach number inlets on turbofan engines are also discussed.

Apparatus and Procedure

Facility Description

The test program was performed at the Engine Noise Test Facility located at Lewis Research Center adjacent to, but sufficiently far from the Flight Research Building so that accurate acoustic measurements could be obtained. The facility is shown schematically in Fig. 1.

The microphone (17) are at the same height as the engine centerline 3.96 meters on a 45.7-meter radius spaced every 10^{o} from the inlet axis to 160^{o}. Also, the reflecting plane is hard pavement. Engine operation is controlled from the flight research building where the noise instrumentation and analysis equipment are located.

Engine Description

The NASA Quiet Engine "C", a low noise technology turbofan demonstrator, was designed, built, and acoustically evaluated under the NASA/GE Experimental Quiet Engine Program. The 97 900-newton (22 000-lb) thrust class turbofan consisted of a newly developed, high tip speed, single-stage fan. It was designed, at the altitude cruise condition, for a corrected tip speed of 472 m/sec (1550 ft/sec) at a bypass pressure ratio of 1.6, and with a corrected fan flow of 415 kg/sec (915 lb/sec). The fan had 26 unshrouded rotor blades and 60 outlet guide vanes. Further details are presented in Ref. 8.

High Throat Mach Number Inlet Design

The selection of the final design concept of the inlet was based upon the noise reduction potential, the aerodynamic performance potential, and considerations of the required mechanical design complexity, weight, sealing problems, and ease of controllability. The final selection of the contracting cowl concept was deemed to be a viable, flight-worthy variable-geometry inlet concept for a CTOL application. A photograph of the takeoff configuration is presented in Fig. 2.

The final aerodynamic contours are presented in Fig. 3. The flight cowl and the cruise contour are shown as dashed lines since neither was tested. A small bellmouth or static test lip was provided in order to approximate the throat flow conditions to be expected at the takeoff and approach flight conditions.

The high throat Mach number inlet front view presented in Fig. 4 indicates the radial panel positions for the approach, takeoff, and cruise positions. The 12 wedges are designed to minimize leakage as the constant-width panels move radially between the approach and cruise positions. In the approach position, only the wedge tips, half circular in cross-section and about 1.3 cm wide remained on the stream at the throat plane. In the takeoff position, the wedge cross-sections block only 2.24 percent of the total throat area.

Shown in Fig. 5 are the three design conditions which were finalized, cruise, takeoff, and approach with an open fan nozzle. The fan nozzle was opened as far as practicable for the approach position in order to reduce the throat area variation required from 46 to 33 percent of the cruise area. An average throat Mach number of 0.865 was selected as the design point for takeoff and approach and test variables were set so that both inlet configurations could be tested over a range of throat Mach numbers from about 0.25 to choked flow conditions by varying corrected fan speed.

Presented in Fig. 6 are the contour area ratios of the two configurations tested as a function of the distance upstream of the fan leading edge. The equivalent conical diffusion angles are 9° and $12\frac{1}{2}^{\circ}$ for the takeoff and approach configurations, respectively. A conventional design equivalent conical diffusion angle for a fixed geometry subsonic CTOL (DC10) inlet is about 11°.

The fixed-position hardware used herein was designed so that the wedges could be removed and that either hard panels or acoustic suppression panels could be tested. A schematic of the acoustic panels is presented in Fig. 7. The same acoustic panels were used in both the approach and takeoff configurations. The acoustic design selected had been previously utilized in tests of NASA Quiet Engine "C". [8]

The contracting cowl inlet installed on Quiet Engine "C" at the NASA Noise Facility is shown in Fig. 8.

Experimental Methods

Aerodynamic and acoustic data were obtained over a range of corrected fan speeds of 43 to 97 percent of design for the takeoff configurations of the high throat Mach number inlet and 43 to 72 percent for the approach configurations.

The acoustic instrumentation and data recording system had a flat response over the frequency range of interest (50 to 20 000 Hz). Data signals were FM recorded from all channels simultaneously on magnetic tape. Each of the three samples for a given corrected fan speed was reduced separately by using a 1/3-octave-band analyzer. The resulting sound pressure levels were arithmetically averaged, adjusted to standard day atmospheric conditions and side-line perceived noise levels were calculated using the standardized procedures presented in Ref. 9.

Aerodynamic instrumentation was located in planes identified in Fig. 9. The pressures, temperatures, and other outputs were received as millivolt signals by the facility data system, digitized and transmitted from a local minicomputer to a remote data collector system by land-line. A large laboratory computor then reduced the data to appropriate aerodynamic parameters. Some data from the traversing probes (fan inlet instrumentation planes) were reduced in the facility minicomputor and final data on air flow, Mach number, velocity, pressure recovery and total pressure distortion were produced.

Some in-duct acoustic data were obtained using traversing probes at the aforementioned fan inlet instrumentation plane and also at the fan-outlet bypass duct plane located about 15 cm downstream of the fan outlet guide vanes.

Surface Mach numbers were calculated from the wall static pressures and the ambient total pressure. Thrust was measured with a load cell and corrected for the axial component of the forward quadrant wind inlet momentum.

Total pressure recovery was calculated first by integrating the total pressure probe traverses in and out for both probes. The results were averaged except for the configurations with wedges (configurations 1 and 3). These total pressures were weighted according to the total percent area blockage of the wedges at the throat (approx. 2.2 percent). The resulting total pressure at the fan inlet plane was then divided by the ambient pressure to yield recovery.

For the computation of total pressure distortion $\mathcal{S}_{max}$ at the fan inlet instrumentation plane, the traversing total pressure was used and the outer 10 percent of the annulus was excluded in determining the minimum pressure (five element equal-area-weighted convention).

Results and Discussion

The aerodynamic results are presented in terms of inlet recovery and distortion parameter as functions of one-dimensional throat Mach number. Experimental

surface Mach number distributions are compared to analytical program results.[7] Measured corrected thrust values are also presented as a function of corrected fan speed.

The acoustic results are presented in terms of 305-meter sideline Perceived Noise Level at a 60° forward angle. Combined aerodynamic and acoustic results are characterized in terms of inlet recovery as a function of acoustic suppression at the 60° forward angle. Some operational problem aspects of using high throat Mach number inlets on turbofan engines are also discussed.

Aerodynamic Performance

Typical total and static pressure profiles measured at the fan inlet instrumentation plane are presented in Fig. 10 for the takeoff configuration 1, for a calculated average throat Mach number of 0.866 and a corrected thrust of 97 900 newtons (takeoff). The pressure traverses for configuration 3 (hard) are not presented but are exactly the same (within instrumentation accuracy) as configuration 1 (soft). The traverses between the wedges (Fig. 10(a)) indicate a boundary layer of about 8 cm in thickness. The traverses behind the wedges (Fig. 10(b)) indicate a thicker combined wake and boundary layer which extends about 12 cm from the wall. The boundary layer rake data at the fan inlet instrumentation plane (not presented) confirmed the total pressure trends at the outer 14 cm of the flow passage. The average of the two total pressure traverses from Fig. 10(a) is shown for reference. The peak in both total and static pressures at 34 cm from the wall is believed to result from the ground vortex which is visible at high fan speeds under certain atmospheric conditions. The vortex was apparently not encountered by the probe on its inward traverse. This result is not surprising that it meanders continually during engine operation.

Typical total and static pressure profiles for the approach configuration (4) measured at the fan inlet instrumentation plane are presented in Fig. 11. The calculated one-dimensional throat Mach number for these profiles is 0.73 and the corrected thrust is about 44 000 newtons. The boundary layer thickness at this condition is about 20 to 24 cm and the almost total lack of airflow in the outer 4 cm (Fig. 11(a)) indicates an incipient total separation condition. The traverses at the top of the inlet (Fig. 11(a)) indicate a more marginal flow condition than the bottom of the inlet (Fig. 11(b)) as evidenced by lower flow (less dynamic pressure) in the outer 30 cm of the flow passage. The difficulty in maintaining engine steady-state conditions is evidenced by the separation of the pressure traces during the 2 minutes required to traverse both directions as shown in both Figs. 11(a) and (b).

To better evaluate the effects of these high throat Mach number inlet configurations on pressure recovery and distortion, typical static and total pressure profiles at the fan inlet instrumentation plane for a baseline cylindrical inlet are presented in Fig. 12. The calculated throat Mach number is 0.22 and the corrected thrust is equal to takeoff. The boundary layer thickness is about 4 cm (much thinner than Figs. 10 and 11) and the pressure traces are very smooth in comparison to Figs. 10 and 11. Obviously, contoured inlets with equivalent conical diffusion angles from 9° (takeoff) to $12\frac{1}{2}^{\circ}$ (approach) produce significantly higher flow distortions than cylindrical inlets at static test conditions.

The comparisons of potential flow analyses[7] with experimental data for the takeoff and approach contours are presented in Fig. 13. The data for the takeoff contour (Fig. 13(a)) closely agree with the calculated wall Mach numbers for a data point whose calculated throat Mach number equaled the analytical choking average throat Mach number of 0.92. The data points downstream of the throat fall above the analysis results because the increase in boundary layer thickness and the resulting increase in average Mach number was not included in the analytical curves. It is seen that the flow is supersonic over a significant area in the region of the throat.

The data for the approach contour (Fig. 13(b)) follow the analysis from the highlight until a few centimeters upstream of the throat. The peak wall Mach number is not reached until about 20 cm downstream of the throat for the highest corrected fan speed data points. These data also indicate a definite shock formation at this point which can lead to a recovery loss and an intermittent flow separation which will be discussed later. Again, for the reason previously stated, the calculated wall Mach number tends to fall higher than the analysis downstream of the point where the peak wall Mach number is attained.

The inlet recovery is presented as a function of average throat Mach number in Fig. 14. The design-point estimated recovery values are also shown as are the choking throat Mach numbers obtained from the analyses.

There is essentially no difference in the data trends for configurations 1 and 3. The presence of the acoustic suppression surface apparently has no measureable effect on recovery. Configuration 2, without wedges, has a slightly higher recovery because there are no wedge wakes. Since the wedges block only about 2 percent of the throat area, they were not expected to affect overall inlet recovery markedly. Hard choking (which is defined as that average throat Mach number at which no

further flow increase can be obtained with further reduction in downstream pressure) is attained at an average throat Mach number of 0.925 for the takeoff configurations. Further slight increases in fan speed in an attempt to increase flow result only in decreased inlet recovery. At design throat Mach number of 0.865, takeoff design recovery is 0.970; configurations 1 and 3 have recoveries of about 0.986; configuration 2 has a recovery of about 0.988.

For the approach configurations, recovery at throat Mach numbers below 0.5 coincide with the takeoff configurations. However, at throat Mach numbers above 0.68, recovery falls off rapidly from a level of 0.987 to about 0.95 at a Mach number of about 0.74. This rapid falloff occurs because of intermittent flow separation in the inlet. This condition is manifested as a low frequency (1 to 2 Hz) audible rumble and an accompanying intermittent disappearance of the condensation curtain across the throat region which occurs during supersonic shock formations.

It is possible that the aforementioned condition during static tests for the approach configurations is entirely different than that which would occur at a forward velocity comparable to approach flight. Such a difference was reported in Ref. 10 and will be discussed later.

Inlet distortion parameter at the fan inlet instrumentation plane as a function of the throat Mach number is presented in Fig. 15. As would be expected, the distortion behind the wedges is higher than between wedges over the range of Mach numbers below the hard choked condition for the takeoff configurations. Once hard choking Mach number is reached, the distortion parameter rises precipitously.

The approach configuration has a relatively low distortion parameter (less than 0.05) until the throat Mach number exceeds 0.68. The distortion parameter then rises rapidly with throat Mach number until intermittent separation occurs.

The discussion of the inlet's effect on the engine performance would not be complete without some reference to engine corrected thrust levels. Therefore, presented in Fig. 16 are the corrected thrust values for various takeoff configurations (along with the baseline configuration) as functions of corrected fan speed. Within the accuracy of the thrust measurement (±1 percent), none of the configurations are different from the baseline at thrusts less than rated takeoff. The trends do show, however, that configuration 2 (without wedges hard) has somewhat higher thrust at corrected fan speeds above 78 percent of rated. As each configuration reaches "choked" inlet conditions the thrust trend "bends over" with respect to corrected fan speed. The ambient wind speed and direction were observed to affect recovery and thrust to some degree.

Corrected specific fuel consumption results (Fig. 17) do show that the baseline configuration is lower than the other configurations by about 2 percent over the range of corrected fan speeds except where inlet flow conditions approach "choking." However, the cruise contour (which was not tested) is of much more interest to the designer who is trying to coax more range and lower D.O.C. out of his airplane. The lower design throat Mach number (0.7) and the rather conventional diffuser design of the cruise contour should give one confidence that little or no penalty in s.f.c. should be expected with this inlet design.

Acoustic Performance

Far field noise measurements at takeoff thrust are presented in Fig. 18. Sideline Perceived Noise Level PNL is shown as a function of angular position from the inlet for the baseline and the takeoff configurations. The effect of the high throat Mach number inlets is very evident in the forward quadrant. At the 60° angular position, the noise is suppressed as much as 15.5 PNdB. It is also evident that the front quadrant noise is suppressed to the point that the aft end noise is now dominant. Also, note that configuration 2 (without wedges) is about 3 dB noisier than configurations 1 and 3 (with wedges) in the front peak noise angle. This results from the lower throat Mach number and higher throat area for configuration 2 with the wedge blockage missing.

The spectra for the 60° angular position are compared in Fig. 19 for the baseline and configuration 1. The suppression is effective over the entire range of frequencies but is especially effective over the MPT range and at the BPF (2000 Hz).

PNL at the 60° angular microphone position over a range of thrust levels is presented in Fig. 20. Configurations 2 and 3 are both noisier than the baseline at fan speeds up to 75 percent. This is probably due to increased turbulence in the diffuser section of the high throat Mach number inlet upstream of the fan and the increased boundary layer thickness (Fig. 10) compared to the cylindrical inlet (Fig. 12) for the baseline configuration. As the fan speed is raised above 75 percent the increasing Mach number then restricts forward radiated noise dramatically. The acoustic treatment of configuration 1 suppresses forward radiated noise effectively (approx. 5 PNdB) over the entire range of fan speeds up to takeoff thrust level. The measured noise suppression of the high Mach number inlets is effectively limited at fan speeds above 92 percent by a noise "floor" caused by forward radiated aft-end noise.

Far field noise measurements at approach thrust level for the baseline and the approach configurations are compared in Fig. 21. Perceived Noise Level is shown as a function of angular position from the inlet for the baseline and the two approach configurations. Recall that the baseline configuration has a standard fan nozzle area and that the approach configurations have a fan nozzle which was essentially 50 percent greater in area. Therefore, aft end noise comparisons should not be made even though fan jet noise should not be a factor. Configurations 4 and 5 exhibit lower noise than the baseline over the range of angular positions but primarily from 10° to 90°. Suppressions of about 13 to 14 PNdB are observed at 40° to 50°. Again, for these configurations as for the takeoff configurations aft end noise seems to be dominant.

The spectra for the baseline and configurations 4 and 5 at the 60° angular position are compared in Fig. 22. The suppression is effective over the frequency range from 100 to 10 000 Hz and is especially effective in reducing the BPF tone by about 16 dB.

PNL at the 60° angular position over a range of corrected fan speeds is presented in Fig. 23. Configuration 4 is noisier than the baseline at corrected fan speeds lower than 65 percent of design for reasons as previously noted for configurations 2 and 3. At higher fan speeds the increasing throat Mach number effectively suppresses forward radiated far-field noise. The treatment of configuration 5 effectively suppresses far field noise over the range of speeds below 65 percent. At speeds higher than 65 percent, the accelerating flow through the inlet then causes noise suppression comparable to configuration 4.

PNL reduction from the baseline configuration at a forward angle of 60° is plotted as a function of inlet recovery in Fig. 24. The superior noise reduction of configuration 1 at high values of inlet recovery is clearly evident.

All the takeoff configurations exhibited maximum PNL reductions from the baseline of about 17 dB. These maximum measured reductions were limited by forward radiated aft-end noise. The accompanying inlet recoveries were above 0.98, and the maximum distortions in the wedge wakes were about 9 percent (Fig. 15), and between wedges, $4\frac{1}{2}$ percent.

The approach configurations exhibited maximum PNL reductions from the baseline of about 12 dB. The recovery was about 0.955 at this condition and the incipient flow separation in the inlet proved to be a marginally safe engine operating condition. This low inlet recovery which was noted previously is even more noticeable in this plot of aeroacoustic performance. Referring to Fig. 25 (Fig. 6 (10)), the effect of increasing the forward velocity from 0 to 41 m/sec at a 12-dB reduction in noise raised the inlet recovery $1\frac{1}{2}$ percent for a translating centerbody type of approach configuration. Increasing the recovery of the configuration reported herein by $1\frac{1}{2}$ percent would result in attainment of the design goal recovery of 0.97. A similar inlet instability was associated with the Ref. 10 configuration at static conditions. This condition was ameliorated also by the increase in forward velocity to 41 m/sec.

By operating the takeoff configuration 1 (Fig. 24) with acoustic treatment at approach thrust, a PNL reduction of about 5.0 dB can be achieved with an inlet recovery of 0.997 and a distortion of less than 3.0 percent (Fig. 15).

Summary of Important Conclusions

1. The takeoff configurations exhibited maximum PNL reductions from the baseline of about 17 dB at an angle of 60° from the inlet measured on a 305-meter sideline. These maximum measured reductions were limited by forward-radiated aft-end noise. The accompanying inlet recoveries were above 0.98.

2. The approach configuration exhibited maximum PNL reductions from the baseline of about 12 dB at an angle of 60° from the inlet measured on a 305-meter sideline. The accompanying recovery was about 0.95 and the incipient flow separation in the inlet proved to be a marginally safe engine operation at static test conditions.

3. By operating the takeoff configuration (with acoustic treatment) at approach thrust, a PNL reduction of about 5.0 dB can be achieved with an inlet recovery of 0.997 and a distortion of less than 3.0 percent.

4. The contracting cowl high Mach number inlet has been shown to be an attractive means to reduce forward radiated noise from a high bypass ratio turbofan engine.

Concluding Remarks

The results of this investigation alone may be misconstrued without reference to results from some small scale inlet tests reported in Ref. 10. The effects of freestream velocity and incidence angle on aeroacoustic performance of high throat Mach number inlets can be significant.

Even though the mini-bellmouth inlet used during this investigation was designed to provide an inlet flow which would approximate the flight conditions of approach and takeoff, changes in ambient wind direction and speed during tests affected inlet performance. The aeroacoustic performance and operational characteris-

tics of the "marginal" approach configuration could be appreciably enhanced by the effect of forward velocity.

Therefore, the unmistakable conclusion to be reached is that in any development program effects such as forward velocity and angle of incidence be determined along with full scale engine tests such as those reported herein.

Symbols

A_e	fan nozzle exit area
A_t	inlet minimum area (throat area)
APP	approach flight condition
BPF	blade passing frequency
D_f	fan tip diameter
D_{hl}	inlet highlight diameter
Φ_{max}	inlet total pressure distortion (maximum pressure - minimum pressure)/average pressure
dB	decibel
F_n/δ	corrected net thrust
Hz	Hertz (cycles per second)
L	inlet length from highlight to diffuser exit
L. E.	leading edge
$\overline{M}_t$	average throat Mach number
M_w	wall Mach number
$N_f/\sqrt{\theta}$	corrected fan speed
PNdB	perceived noise decibel
PNL	perceived noise level, dB
P_0	freestream total pressure
P_1	diffuser exit total pressure
R	radius
R_{fan}	fan tip radius
R_{HL}	inlet highlight radius
R_{hub}	fan hub radius
R_{max}	flight cowl maximum radius
R_t	inlet throat radius
T.O.	takeoff flight condition
X	axial distance measured from highlight
α	incidence angle
δ	freestream corrected total pressure
η_R	recovery factor (total pressure at fan inlet/ambient pressure)
θ	inlet corrected temperature

References

1. Sullivan, T. J., Youngblans, J. L., and Little, D. R., "Single Stage, Low Noise, Advanced Technology Fan. Vol. 1, Aerodynamic Design. NASA CR-134801, Mar. 1976.

2. Chestnutt, D., "Noise Reduction by Means of Inlet-Guide-Vane Choking in an Axial-Flow-Compressor," NASA TN D-4682, July 1968.

3. Lumsdaine, E., "Development of a Sonic Inlet for Jet Aircraft," Internoise '72 Proceedings; International Conference on Noise Control Engineering, Institute of Noise Control Engineering, Poughkeepsie, N. Y., 1972, pp. 501-506.

4. Klujber, F., "Development of Sonic Inlets for Turbofan Engines," Journal of Aircraft, Vol. 10, Oct. 1973, pp. 579-586.

5. Savkar, S. D. and Kazin, S. B., "Some Aspects of Fan Noise Suppression Using High Mach Number Inlets," Journal of Aircraft, Vol. 12, May 1975, pp. 487-493.

6. Kazin, S. B., "High Tip Speed Fan Inlet Noise Reduction Using Treated Inlet Splitters and Accelerating Inlets," R72AEG336, Aug. 1973, General Electric Co., Cincinnati, Oh; also NASA CR-121268.

7. Albers, J. A. and Stockman, N. O., "Calculation Procedures for Potential and Viscous Flow Solutions for Engine Inlets," ASME Paper 74-GT-3, Zurich, Switzerland, 1974.

8. Kazin, S. B. and Pass, J. E., "NASA/GE Quiet Engine "C" Acoustic Test Results," R73AEG364, Apr. 1974, General Electric Co., Evendale, Oh., also NASA CR-121176.

9. Montegani, F. J., "Some Propulsion System Noise Data Handling Conventions and Computer Programs Used at the Lewis Research Center," NASA TM X-3013, Mar. 1974.

10. Miller, B. A., "Experimentally Determined Aeroacoustic Performance and Control of Several Sonic Inlets," AIAA Paper 75-1184, Anaheim, Calif., 1975.

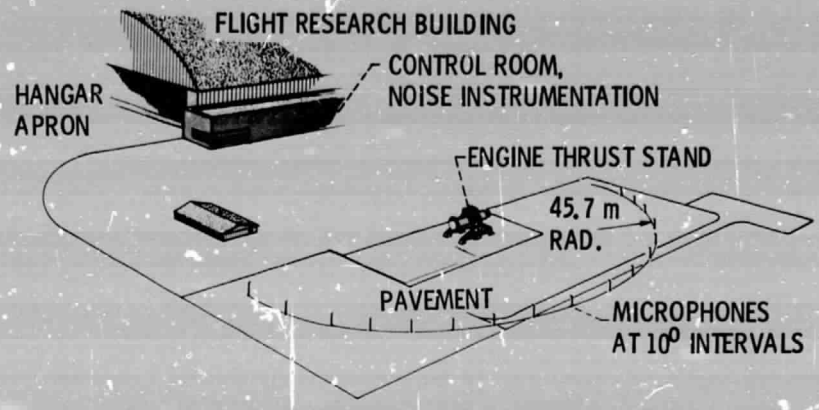

Figure 1. - Engine Noise Test Facility plot plan showing thrust stand, microphone array, control and noise instrumentation rooms.

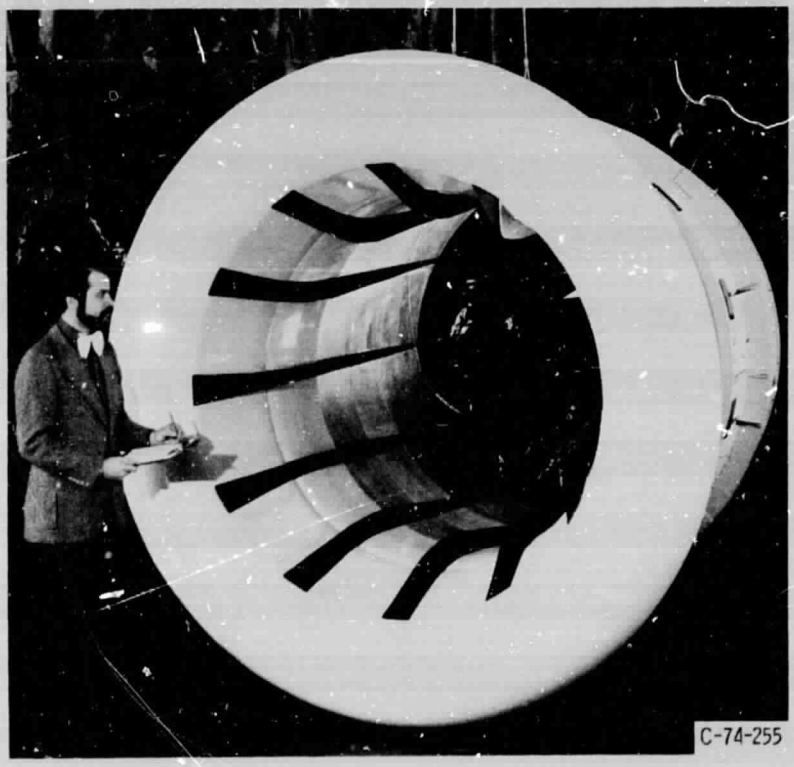

Figure 2. - Takeoff configuration showing the twelve wedges.

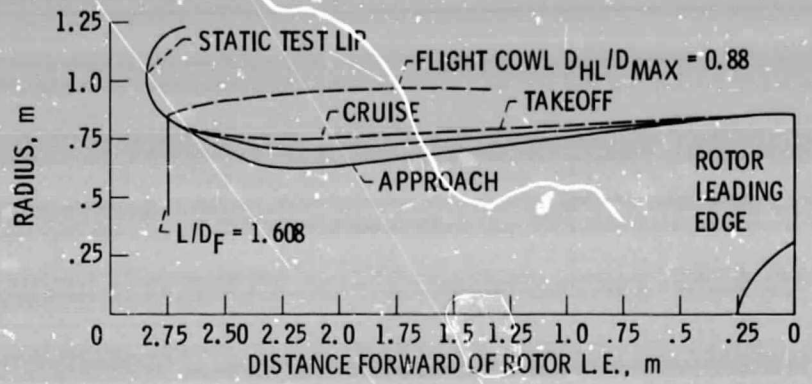

Figure 3. - Contracting-cowl high-throat-Mach-number inlet showing internal contour for various flight conditions and the static test lip utilized for performance evaluation.

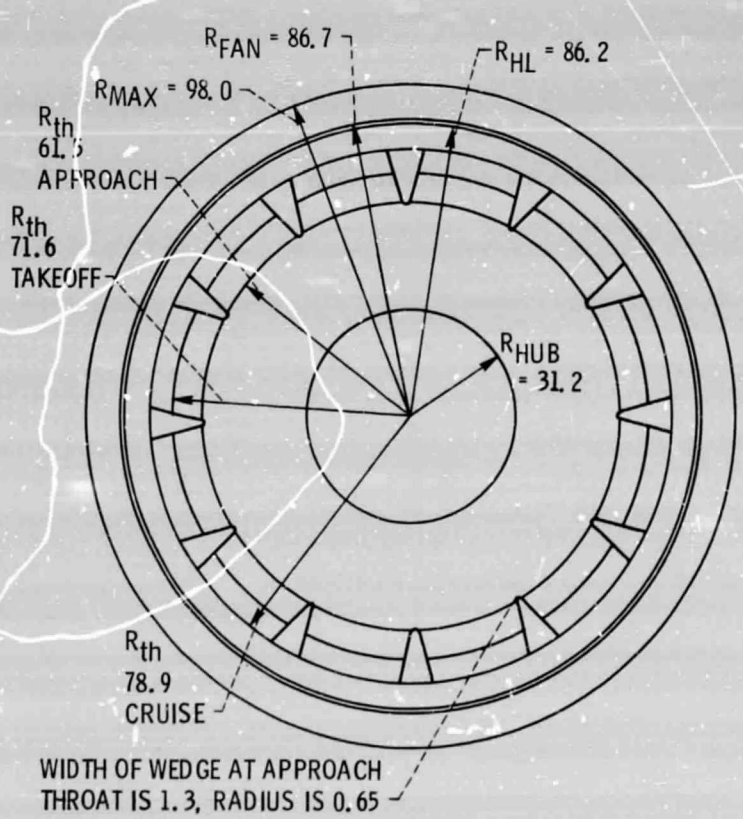

Figure 4. - Contracting-cowl high-Mach-number inlet front view showing throat section and other key radii. (Note: all dimensions are in cm.)

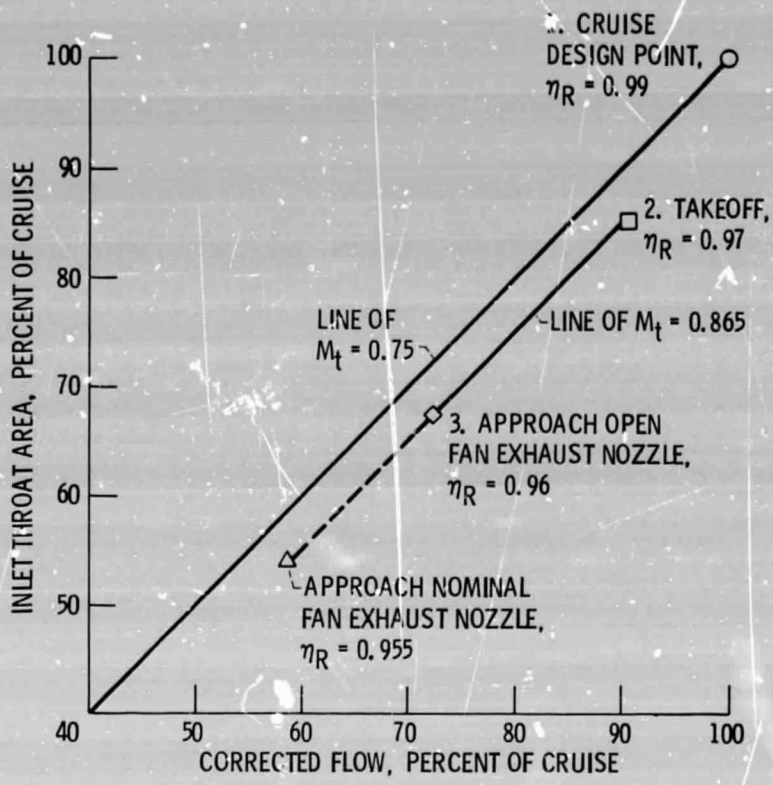

Figure 5. - Inlet parameter plot with design points and estimated recoveries indicated.

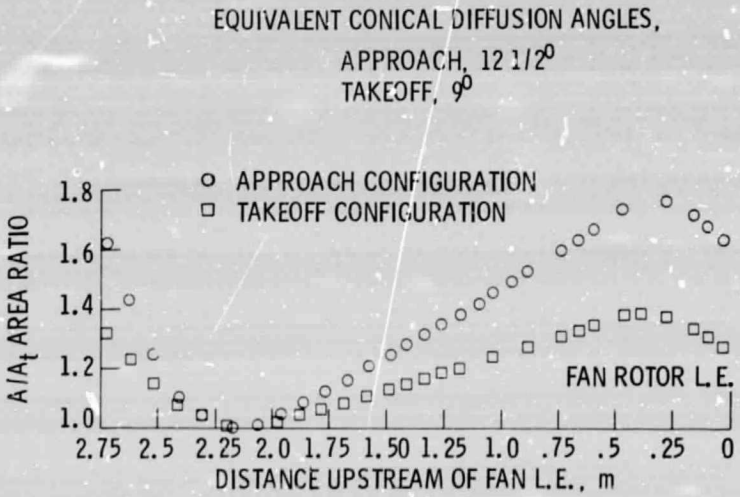

Figure 6. - Design contour area ratios for approach and takeoff configurations.

	B'KING DEPTH	FACING SHEET		
		THICKNESS	HOLE DIAM.	% OPEN
A	0.76	0.08	0.14	7.3
B	2.54	.08	.14	10.0
C	7.19	.08	.14	2.5
D	2.79	.13	.13	7.0

NOTE: ALL DIMENSIONS ARE IN CM.

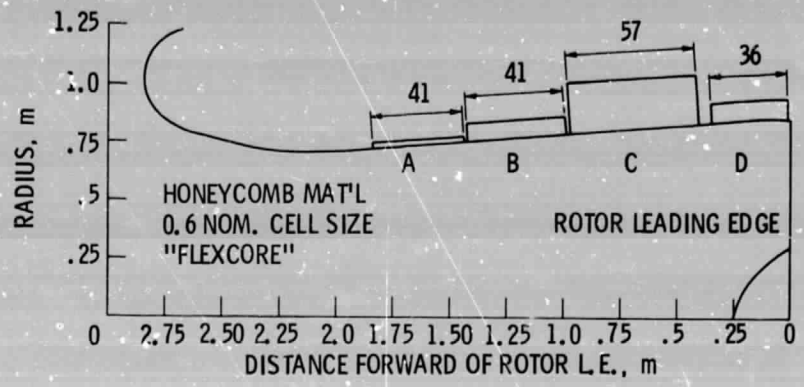

Figure 7. - Acoustic treatment definition for the contracting cowl high throat Mach number inlet.

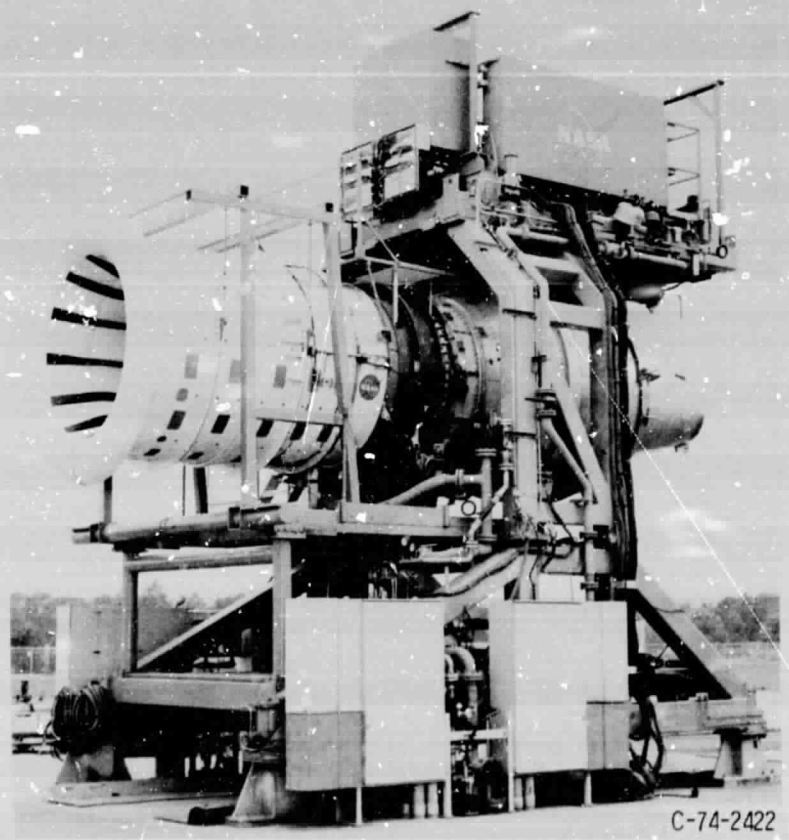

Figure 8. - High throat Mach number inlet installed on engine "C" at the Engine Noise Test Facility.

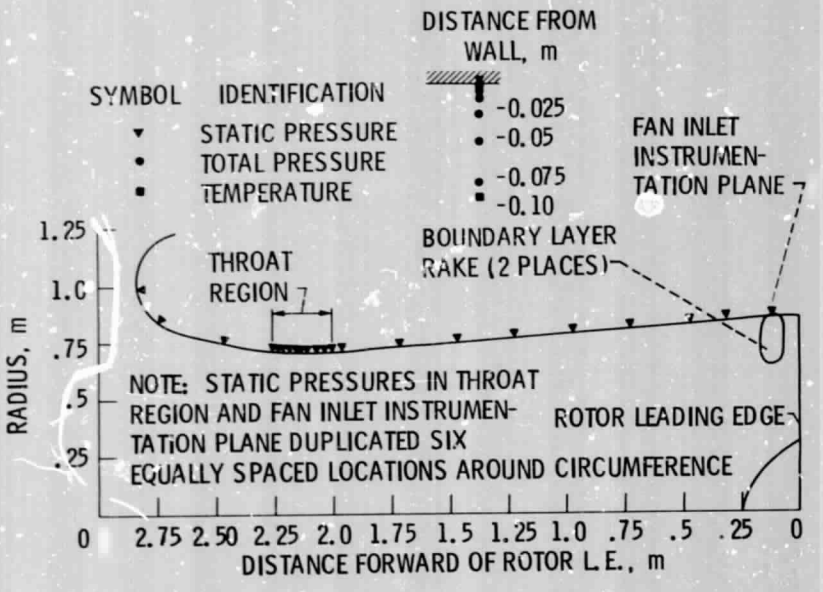

Figure 9. - High throat Mach number inlet instrumentation.

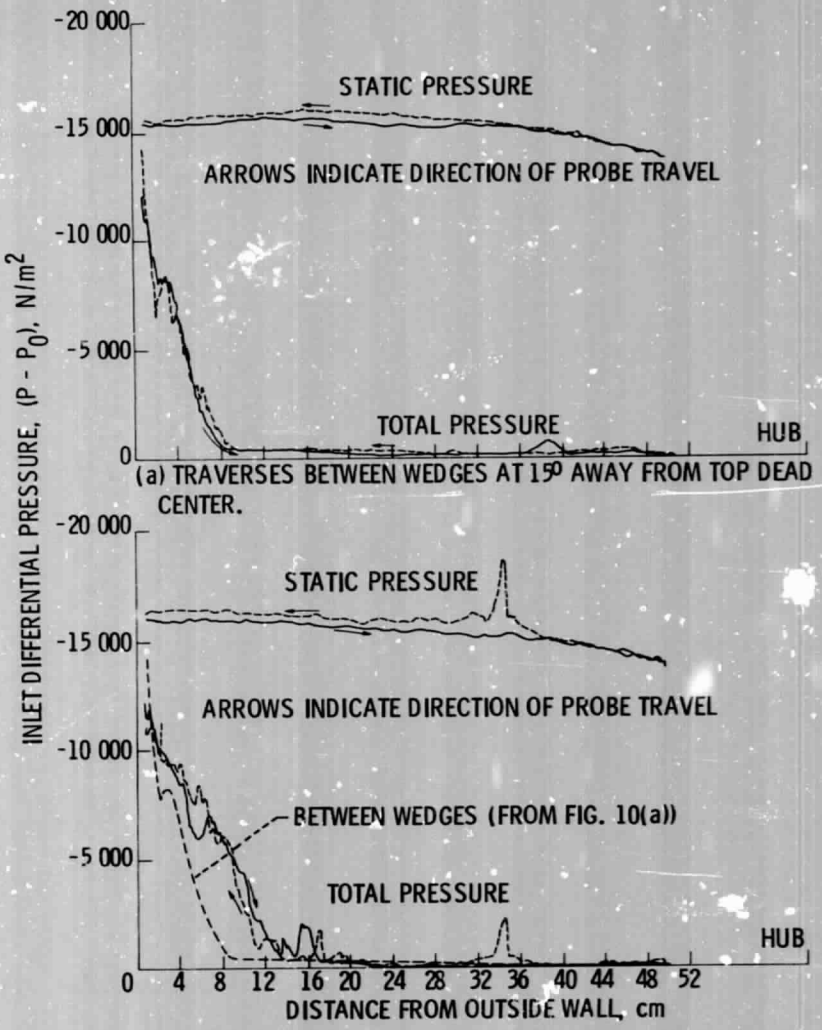

(a) TRAVERSES BETWEEN WEDGES AT 15° AWAY FROM TOP DEAD CENTER.

(b) TRAVERSES BEHIND WEDGES AT 30° ABOVE BOTTOM DEAD CENTER.

Figure 10. - Total and static pressure traverses at the fan inlet instrumentation plane for configuration 1, (takeoff, soft, with wedges).

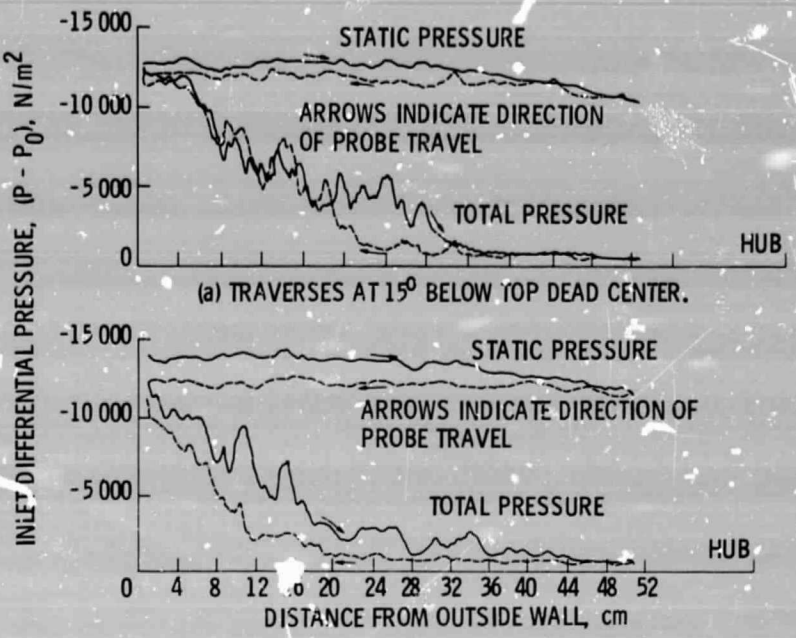

Figure 11. - Total and static pressure traverses at the fan inlet instrumentation plane for configuration 4, (approach, hard).

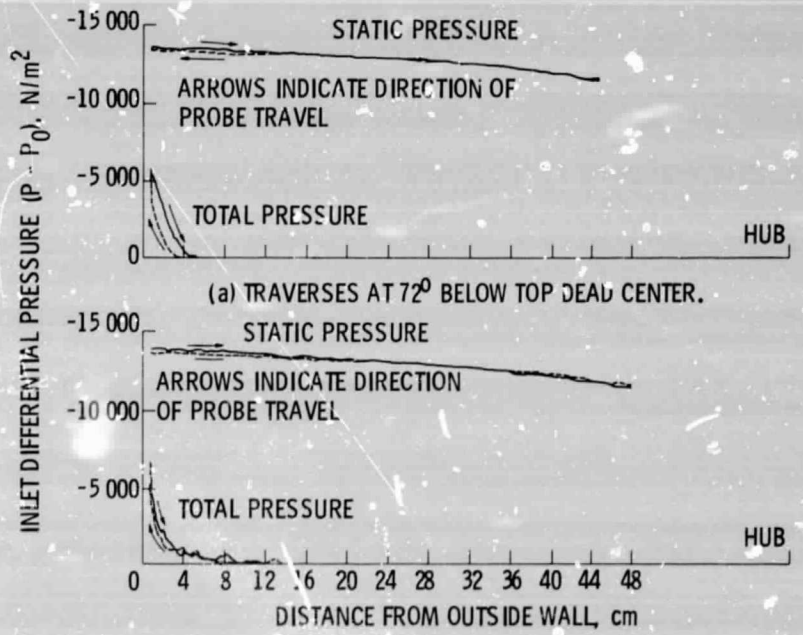

Figure 12. - Total and static pressure traverses at the fan inlet instrumentation plane for baseline configuration, (cylindrical inlet with bellmouth).

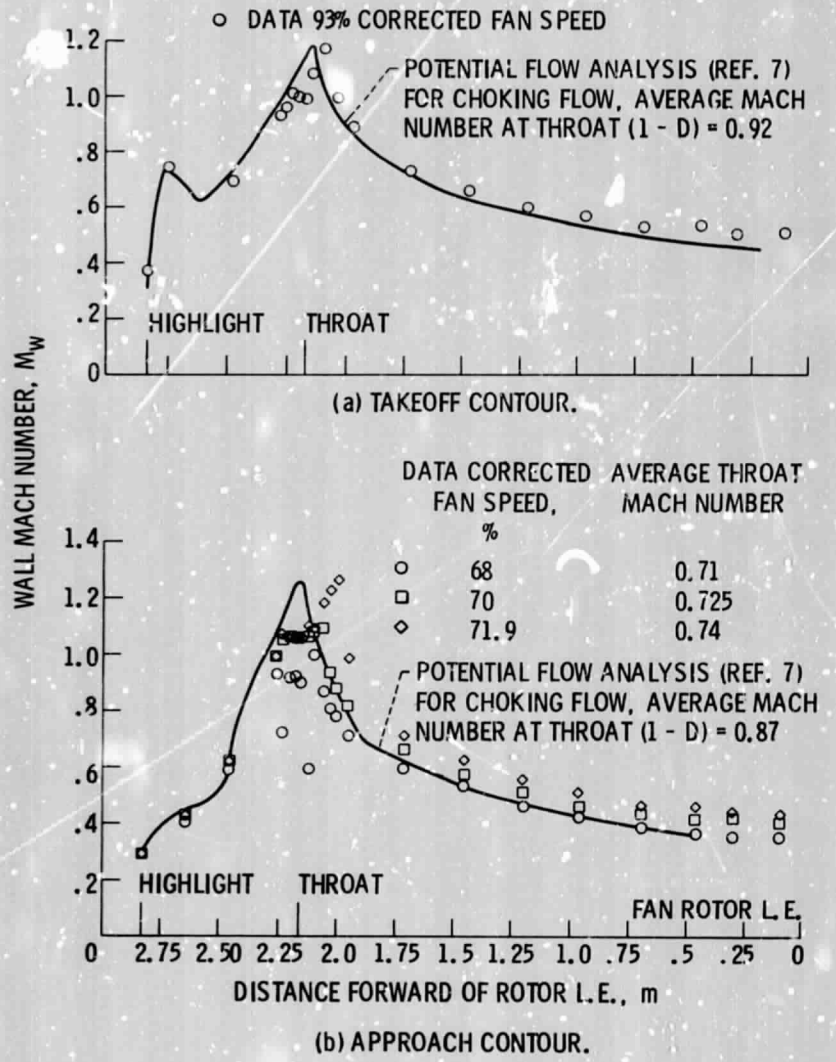

Figure 13. - Comparison of experimental data with potential flow analysis.

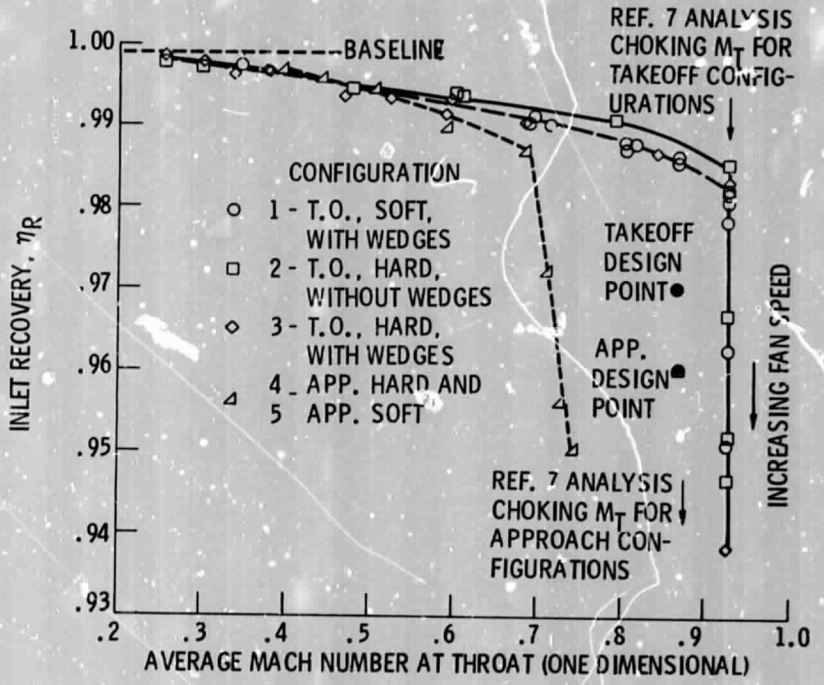

Figure 14. - The variation of inlet recovery with average Mach number at the throat for all configurations.

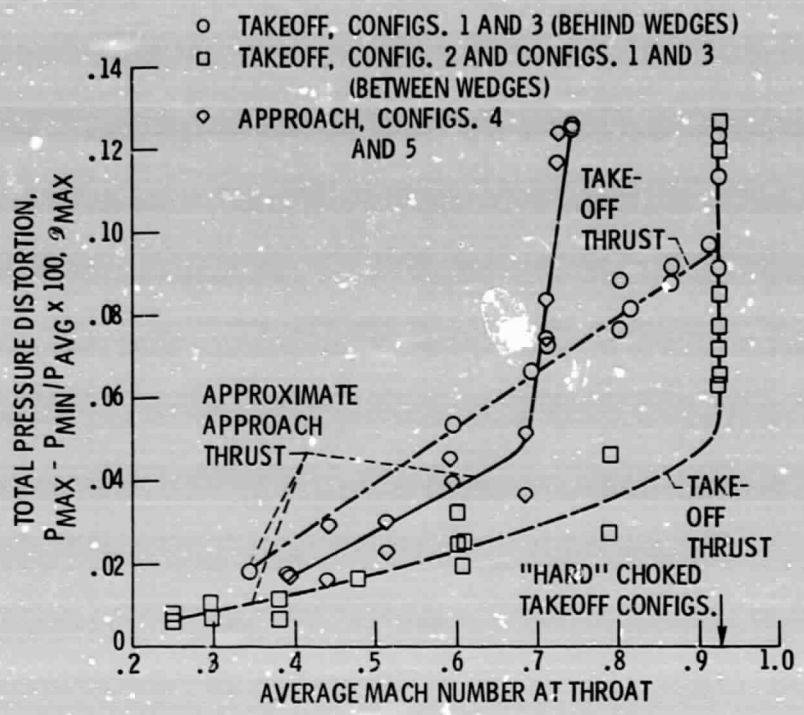

Figure 15. - The variation of inlet distortion with average Mach number at the throat for all configurations.

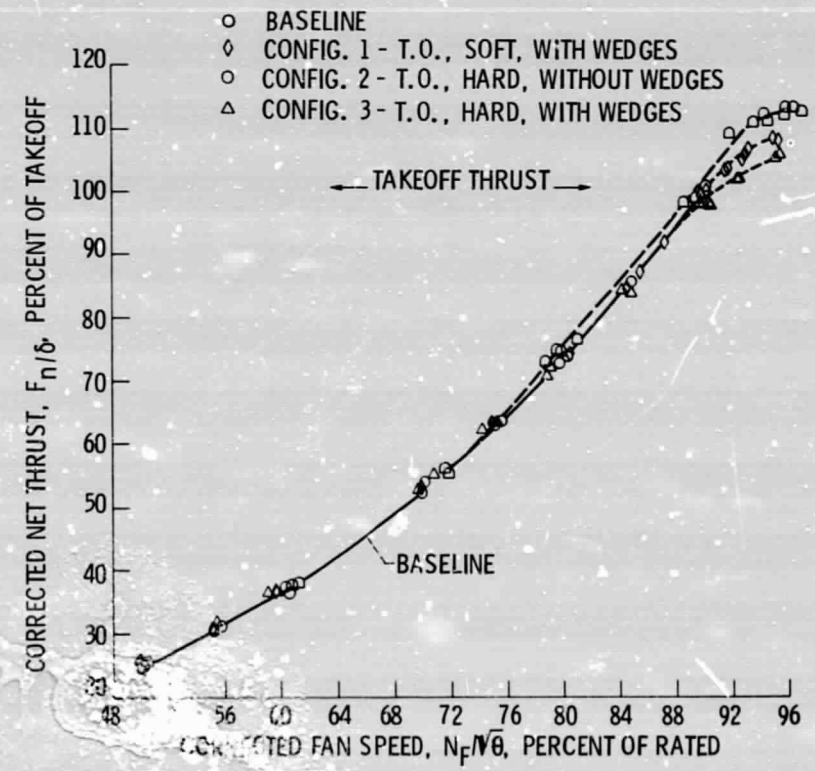

Figure 16. - Effect of inlet configuration on variation of corrected thrust with corrected fan speed.

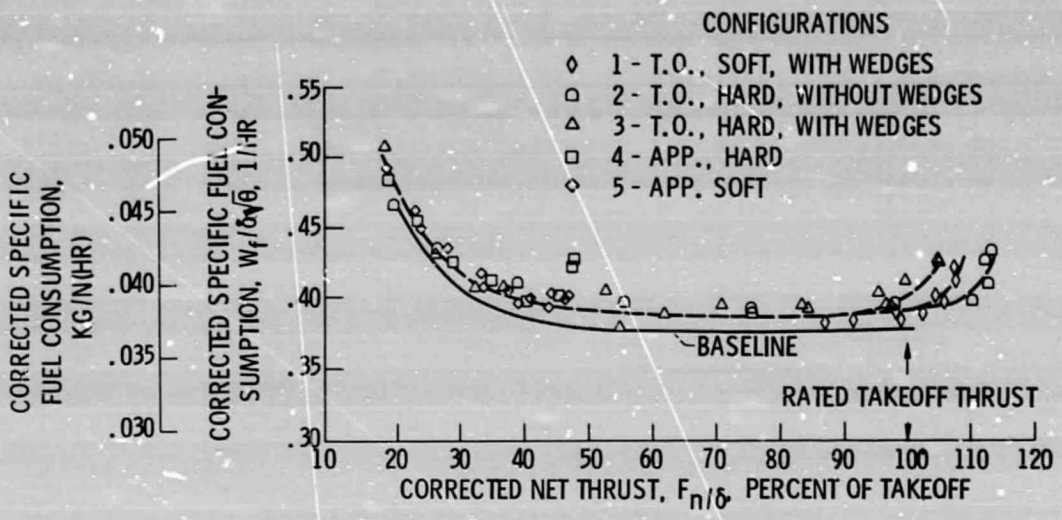

Figure 17. - Effect of inlet configuration on variation of corrected specific fuel consumption with corrected net thrust.

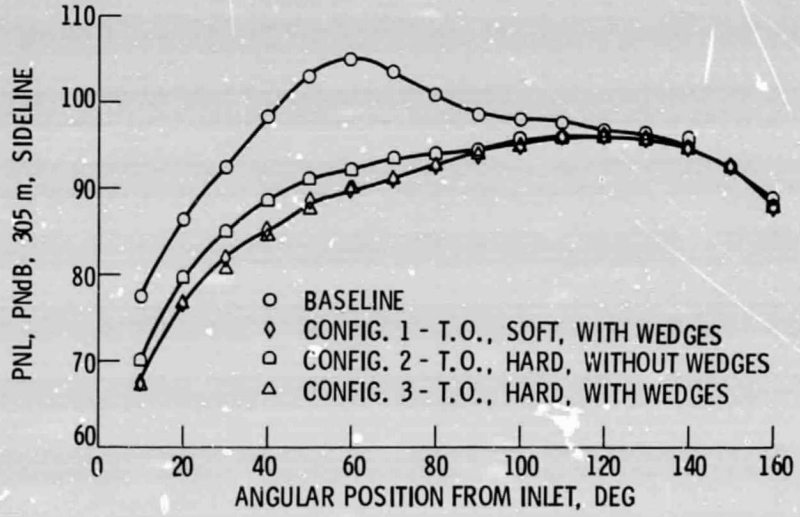

Figure 18. - Comparison of PNL directivities for baseline and takeoff configurations at takeoff thrust level.

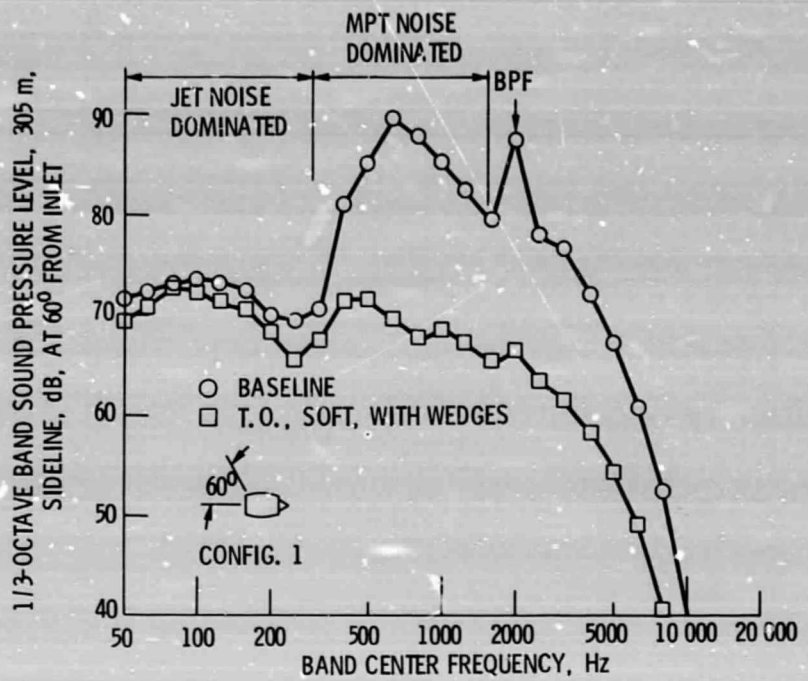

Figure 19. - Comparison of SPL spectra for baseline and takeoff configuration at takeoff thrust level.

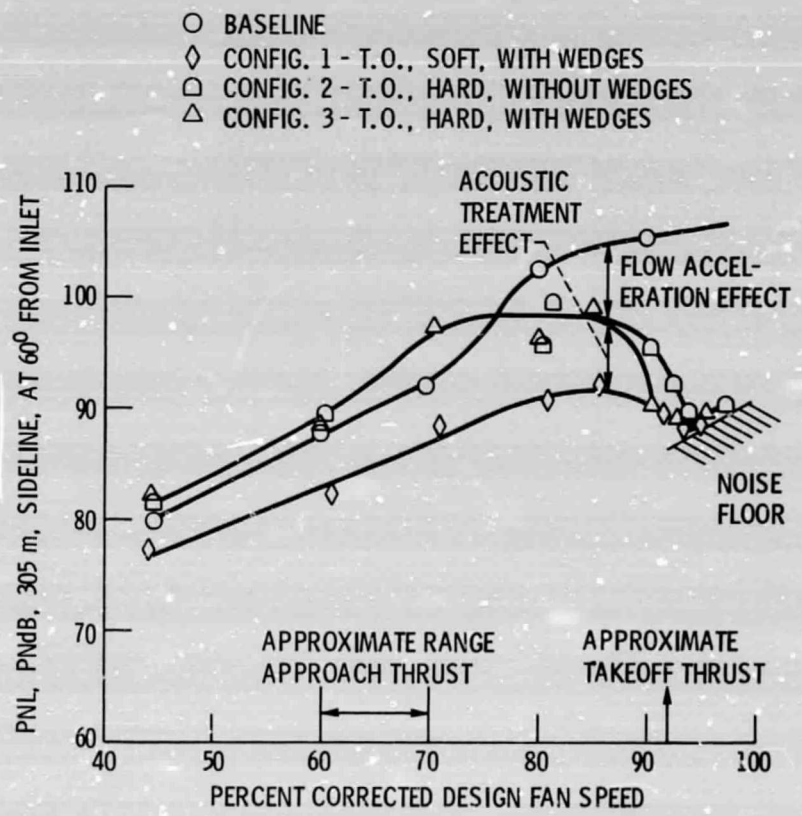

Figure 20. - Comparison of PNL at the 60° position for baseline and takeoff configurations.

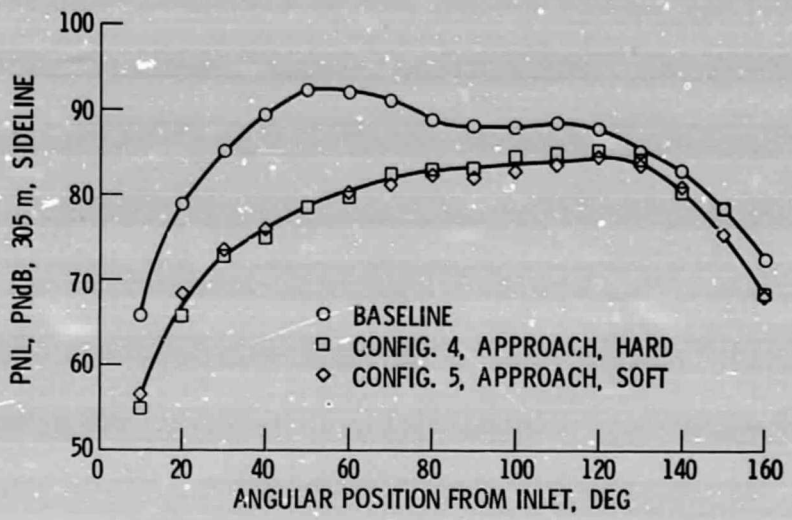

Figure 21. - Comparison of PNL directivities for baseline and approach configurations at approach thrust level and 70% corrected design fan speed.

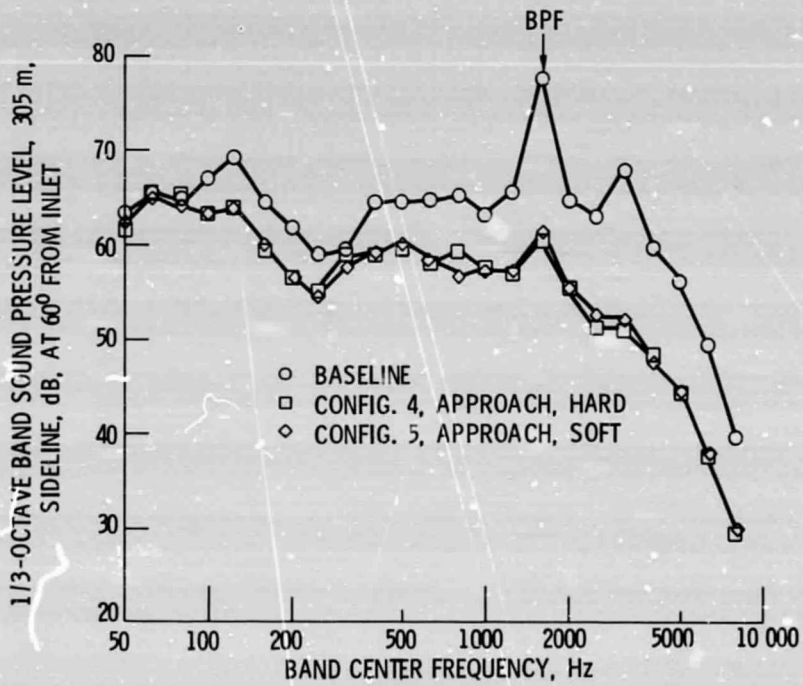

Figure 22. - Comparisons of SPL spectra for baseline and approach configurations at approach thrust level and 70% corrected design fan speed.

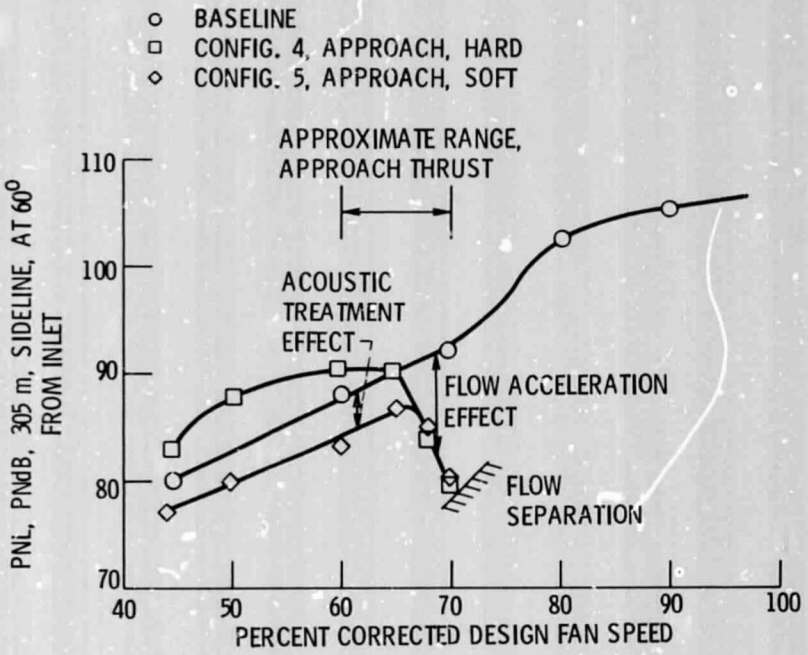

Figure 23. - Comparison of PNL at the 60° position for baseline and approach configurations over a range of corrected design fan speeds.

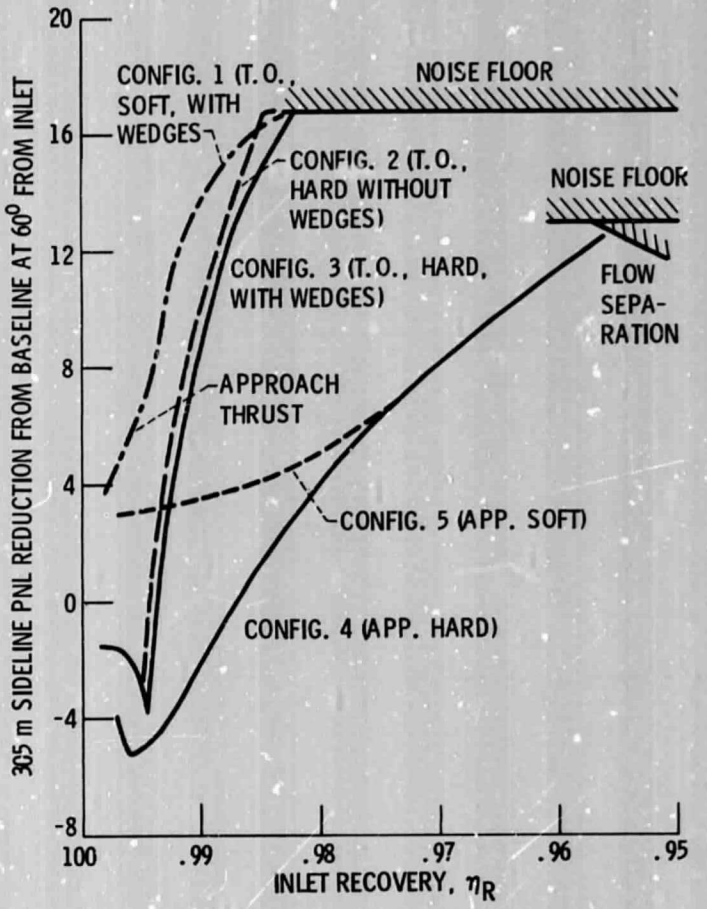

Figure 24. - PNL reduction as a function of inlet recovery, takeoff and approach configurations.

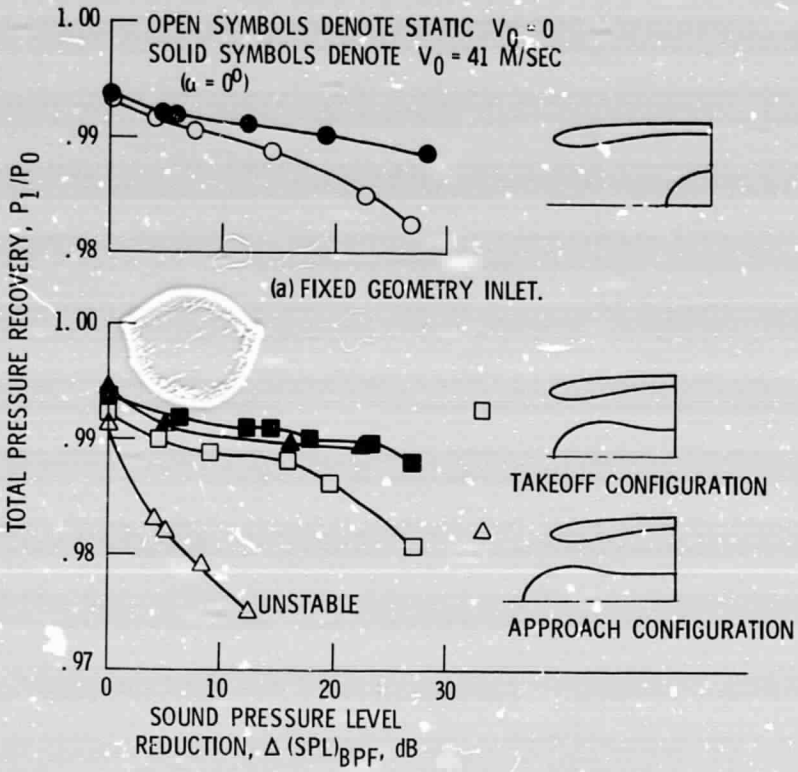

(b) TRANSLATING CENTERBODY INLET WITH SHORT DIFFUSER.

Figure 25. - Effect of free stream velocity on inlet performance.